THE WIDTH OF A SOLAR CORONAL MASS EJECTION AND THE SOURCE OF THE DRIVING MAGNETIC EXPLOSION

Ronald L. Moore, Alphonse C. Sterling, and Steven T. Suess

Space Science Office, VP62, Marshall Space Flight Center, Huntsville, AL 35812

26 January 2007

To be submitted to

The Astrophysical Journal

ABSTRACT

We show that the strength of the magnetic field in the area covered by the flare arcade following a CME-producing ejective solar eruption can be estimated from the final angular width of the CME in the outer corona and the final angular width of the flare arcade. We assume (1) the flux-rope plasmoid ejected from the flare site becomes the interior of the CME plasmoid, (2) in the outer corona ($R > 2R_{Sun}$) the CME is roughly a "spherical plasmoid with legs" shaped like a light bulb, and (3) beyond some height in or below the outer corona the CME plasmoid is in lateral pressure balance with the surrounding magnetic field. The strength of the nearly radial magnetic field in the outer corona is estimated from the radial component of the interplanetary magnetic field measured by Ulysses. We apply this model to three well-observed CMEs that exploded from flare regions of extremely different size and magnetic setting. One of these CMEs is an over-and-out CME that exploded from a laterally far offset compact ejective flare. In each event, the estimated source-region field strength is appropriate for the magnetic setting of the flare. This agreement (1) indicates that CMEs are propelled by the magnetic field of the CME plasmoid pushing against the surrounding magnetic field, (2) supports the magnetic-arch-blowout scenario for over-and-out CMEs, and (3) shows that a CME's final angular width in the outer corona can be estimated from the amount of magnetic flux covered by the source-region flare arcade.

Subject headings: Sun: coronal mass ejections (CMEs) – Sun: flares – Sun: magnetic fields – Sun: corona

1. INTRODUCTION

All solar flares erupt in initially closed magnetic fields, and all coronal mass ejections (CMEs) erupt from closed-field regions of the Sun (Svestka 1976; Gopalswamy & Thompson 2000). From observations of the form and action of the magnetic field before and during flares and CMEs, it is nearly certain that in all flares and in a large majority if not all CMEs, the pre-eruption field is strongly nonpotential (has a large store of free magnetic energy), and the flare and/or CME is produced by an explosive release of some of the free energy (e.g., Sturrock 1980; Moore et al 1984, 2001; Moore 1987, 1988, 2001; Machado et al 1988; Svestka et al 1992; Canfield et al 1999). While it is widely accepted that most CMEs and all flares are magnetic explosions (and/or implosions (Hudson 2000)), the relation of CMEs to flares remains ambiguous and controversial (Kahler 1992; Gosling 1993; Hudson et al 1995; Harrsion 1995, 2006; Plunkett et al 2001). Often, when a CME occurs together with an underlying flare it is obvious that the flare is produced as a byproduct of the magnetic explosion that produces the CME; this is typically the case for filament-eruption explosions that produce both a CME and a long-duration two-ribbon flare and flare arcade (e.g., Gibson et al 2006; Moore & Sterling 2006). However, if there is no observed ejection, such as an ejective filament eruption, from the flare site, and/or if the flare is far from centered under the CME, it is questionable whether the flare and the CME are produced by the same magnetic explosion or by two separate explosions (e.g., Kahler 1992; Choudhary & Moore 2003; Harrison 2006). If separate, the flare explosion could occur by chance and be unrelated to the CME explosion, or could be triggered by the CME explosion, or could be the trigger of the CME explosion (Machado et al 1988; Moore et al 1999). In this paper, we present a way to assess, from the width of the CME and the area and magnetic location of the flare, whether the CME exploded from the flare site.

This paper stems from observations of streamer-puff CMEs, the new variety of CME recently found by Bemporad et al (2005). The name "streamer puff" comes from the character of these CMEs in coronagraph movies: like a streamer-blowout CME (Howard et al 1985), a streamer-puff CME erupts from the base of a coronal streamer and travels out along the streamer, but in contrast to a streamer-blowout CME, a streamer-puff CME only transiently inflates the streamer, leaving the streamer only slightly changed after passage rather than obliterated. From observations from the Solar and Heliospheric Observatory (SOHO) of a homologous sequence of streamer-puff CMEs and synchronous compact ejective flares that occurred in a streamer rooted near the limb, Bemporad et al (2005) found clear evidence that the source of the driving magnetic explosion in streamer-puff CMEs is different from that in streamer-blowout CMEs. A streamer-blowout CME is driven by the ejective eruption of a flux rope (often carrying a filament) from the sheared-field core of the streamer-base arcade, that is, from along much of the length of the magnetic inversion line (neutral line) of the streamer arcade (e.g. Low 1996; Gibson et al 2006). In contrast, each of the streamer-puff CMEs observed by Bemporad et al was evidently the consequence of a compact ejective flare in the flank of the streamer arcade, far from the arcade's inversion line. The flares occurred at the edge of a small island of opposite-polarity flux in the streamer base. Presumably, this island was half the flux of a

small bipole (magnetic arcade) that had emerged within the outer domain of the streamer arcade.

Bemporad et al (2005) proposed the following scenario for streamer-puff CMEs. A compact magnetic arcade is embedded in the foot of a high-reaching outer loop of a streamer-base arcade. The core field of the embedded arcade is strongly sheared as in larger arcades that ejectively erupt to produce a CME and two-ribbon flare. In the manner of these larger arcades, the compact arcade erupts, producing a compact flare along with an escaping flux-rope plasmoid. The plasmoid explodes up the leg of the encompassing streamer-arcade loop, guided by the ambient magnetic field. The force of this explosion is strong enough that it blows out the top of the guiding loop, thereby making a streamer-puff CME that travels out along the streamer. This magnetic-arch-blowout scenario is supported by the coronal dimming footprint of a streamer-puff CME found by Moore & Sterling (2007). In this event, coronal dimming was observed at both ends of an outer loop of a large arcade in the base of the streamer. The arcade's sheared core field, traced by a filament, did not erupt: the filament was not disturbed by the dimming event. The dimming in the feet and legs of the outer loop occurred as a compact ejective flare erupted in one end of the loop, during the onset of a streamer-puff CME that traveled out along the streamer, consistent with the loop having been blown out in the production of the CME. Thus, the magnetic setting and the spatial and temporal coordination of the compact ejective flare, coronal dimming, and streamer-puff CME were nicely consistent with the magnetic-arch-blowout scenario.

While the observations of streamer-puff CME events presented by Bemporad et al (2005) and Moore & Sterling (2007) do make a strong case for the magnetic-arch-blowout scenario, this evidence is only morphological and qualitative. The compact ejective flares in the reported events spanned only ~ 10,000 km (or ~ 1° in heliocentric angle), whereas the corresponding streamer-puff CMEs had angular widths of 20°-40°. Is it plausible that such compact eruptions could produce CMEs of so much greater width? This question provoked the work presented in this paper. For a flare that occurs co-temporally and roughly co-spatially with the onset of a CME, the basic premise of this paper is that if the magnetic flux covered by the flare is comparable to the magnetic flux in the CME, then the magnetic explosion that produces the flare is plausibly the magnetic explosion that drives the CME, and, conversely, if the magnetic flux in the CME is much greater than that in the flare, then the flare explosion is not the main driver of the CME. Under this premise, the flare-site magnetic field strength required for the CME to have been driven by the flare explosion can be estimated from the flux content of the CME and the observed area covered by the flare. Agreement between this estimated field strength and the observed field strength at the flare would be a positive indication that the CME exploded from the flare site. If the estimated required field strength in the flare were much stronger than the observed field strength, this would indicate that the CME did not explode from the flare site. To enable this test, we estimate the flux content of a CME from the CME's final angular width in the outer corona. By this method, we find that the 40° width of the streamer-puff CME reported by Moore & Sterling (2007) is consistent with the CME explosion having come from the identified offset compact ejective flare. Of broader importance, our results

indicate that when the magnetic explosion that produces a CME also produces a flare as a byproduct, the observed magnetic flux covered by the flare gives an estimate of the final angular width of the CME in the outer corona.

2. ESTIMATION OF THE MAGNETIC FLUX IN A CORONAL MASS EJECTION

2.1. CME Explosion Model

Our method of estimating the total flux of the magnetic field in a coronal mass ejection is based on the standard concept for the magnetic explosion that produces a CME in tandem with a flare. Over the past three or four decades, modern observations of CME-producing filament-eruption flares (especially coronal images and movies from space together with chromospheric movies and photospheric vector magnetograms from the ground, all with spatial resolution of a few arcseconds or better) have shown that the basic pre-eruption magnetic field is a magnetic arcade (closed bipole) in which the core field is strongly sheared (e.g., Moore & LaBonte 1980; Hagyard et al 1984; Moore & Rabin 1985; Moore et al 1984, 1987, 1999; Machado et al 1988). Whether or not this sheared-core arcade is embedded in surrounding magnetic field that is involved in triggering and unleashing the explosion, the explosion is driven by the expansion of a twisted rope of magnetic field that erupts from the core of the arcade and often carries a filament of chromospheric plasma within it (e.g. Moore 1988, 2001; Antiochos 1998; Moore & Sterling 2006). The observed typical sigmoidal form, eruptive motion, and expansion of the filament-carrying core field before and during eruption are characterized by the so-called standard picture for CME explosions, which was first put forth by Hirayama (1974) and has been modified and further supported by subsequent observations and modeling (Kopp & Pneuman 1976; Heyvaerts et al 1977; Moore & LaBonte 1980; Moore et al 1980, 1991, 1995, 1997, 2001; Sturrock et al 1984; Moore & Roumeliotis 1992; Shibata et al 1995; Rust & Kumar 1996; Shibata 1998; Canfield et al 1999; Sterling et al 2000, 2001a,b,; Sterling & Moore 2001a,b, 2003, 2004a,b, 2005; Rust & LaBonte 2005; Gibson et al 2006; Moore & Sterling 2006).

Sketched in Figure 1 is our version of the standard picture for the three-dimensional topology and reconnection of the magnetic field before and during the explosion of a CME from a sheared-core arcade. Only a few indicative field lines are drawn in these sketches. Before eruption (first panel), a filament is held in the sheared core field. We assume that the filament material resides in dips in field lines (not shown) that run the length of the arcade, rooting at the opposite ends of the core-field sigmoid, as in the model of Antiochos et al (1994). These field lines amount to a pre-eruption flux rope that floats in the core field of the arcade. The middle stretch of this filament-holding sigmoidal flux rope runs between the arms of the two core-field elbows, that is, between the core-field legs that shear past each other in the middle of the arcade, as shown in the first panel. This initial filament-holding flux rope can begin to erupt as a result of any one or any combination of three triggering processes (see Moore & Sterling 2006): (1) internal tether-cutting reconnection between the legs of the sheared core field under the filament-holding flux rope, as shown in the second panel of Figure 1; (2) external tether-cutting reconnection (breakout

reconnection) at a current sheet (not shown in Figure 1) between the envelope of the arcade and oppositely-directed overlying magnetic field; (3) MHD instability/loss of equilibrium without reconnection.

In the concept sketched in Figure 1, regardless of how the eruption of the filament flux rope is triggered, once the eruption is underway, internal tether-cutting reconnection soon begins and continues as in Figure 1, growing the flux rope (adding more flux to it) and further unleashing the erupting core field from its ties to the photosphere (thereby strengthening the explosion) (Moore & Sterling 2006). In a CME explosion, the exploding flux rope overpowers its envelope of less-sheared arcade field, and the arcade is blown out, wrapped around the ejecting flux rope as in the last panel of Figure 1. The stretched legs of the blown-out arcade envelope reconnect in the wake of the ejected flux rope, forming and heating the flare arcade and flare ribbons as in the last panel of Figure 1.

For the CME explosion scenario sketched in Figure 1, the escaping loop of core flux rope and the arcade envelope around it, and any field that arches over the pre-eruption arcade and is also blown out, comprise the total escaping plasmoid that is observed as a CME in the outer corona. In this scheme, the flux traversed by the flare ribbons over the course of the flare is roughly equal to the flux contained in the driving interior plasmoid in the CME, the escaping plasmoid consisting of the ejected flux rope and arcade envelope (Figure 1, last panel). In order for the explosion to become a CME, it seems likely that the flux in the driving plasmoid must exceed the flux in any overarching field that is draped over the driving plasmoid and that forms an outer shell of the total CME plasmoid. If so, for the CME explosion scenario sketched in Figure 1, the flux spanned by the flare arcade and ribbons after flare maximum, Φ_{Flare}, roughly equals the flux content of the CME, Φ_{CME}:

$$\Phi_{Flare} \approx \Phi_{CME}. \quad (1)$$

That is, we expect and assume that $1 \leq \Phi_{CME}/\Phi_{Flare} < 2$.

Many CMEs, especially those centered on a filament eruption, have a characteristic three-part bubble structure consisting of a bright outer shell around a darker interior enclosing a bright core that typically contains the ejected part of a filament (Kahler 2006). In Figure 2, this three-part structure is sketched for a typical CME rooted near the limb, as it would appear in a LASCO C2 coronagraph image when the center of the bright core has reached a heliocentric distance of about 4 R_{Sun} (e.g., see Figure 5 of Kahler 2006). Judging from this observed typical form, we surmise that in the outer corona ($R \sim$ 2-20 R_{Sun}) a typical CME is roughly a "spherical plasmoid with legs," having roughly the three-dimensional shape of a light bulb. This inference is supported by the observation that halo CMEs that are directed nearly along the Sun-coronagraph line are typically roughly circular in coronagraph images (e.g., see Figure 1 of Kahler 2006). In our model CME depicted in Figure 2, the bright core, its dark envelope, and possibly some inner shell of the bright outer envelope, are the expanding continuation of the escaping driving flux-rope plasmoid sketched in the last panel of Figure 1. The outer remainder of the bright envelope is made of the overlying magnetized corona that has been pushed out ahead of and around the driving plasmoid.

In either the ambient corona or the CME plasmoid, the total lateral pressure, p_{Lat} (the total pressure perpendicular to the magnetic field), to first order is the sum of the thermal plasma pressure, $3n_ekT$, and the magnetic pressure, $B^2/8\pi$:

$$p_{Lat} = 3n_ekT + B^2/8\pi, \quad (2)$$

where n_e is the electron number density, k is the Boltzmann constant, T is the temperature, and B is the magnetic field strength. For CMEs that are magnetically driven, we assume that the spatially averaged plasma pressure in the CME is negligible compared to the spatially averaged magnetic pressure. In this case, to a good approximation, the lateral pressure in the CME is given by the average magnetic pressure:

$$p_{Lat,CME} \approx [B_{CME}]^2/8\pi, \quad (3)$$

where B_{CME} is the root-mean-square field strength in the CME. We assume that when the CME plasmoid is new-born in the inner corona ($R <\sim 2R_{Sun}$) its internal pressure exceeds the ambient pressure, causing it to expand laterally as it rises, decreasing its pressure until it is roughly in balance with the ambient lateral pressure, $p_{Lat,Amb}$. We will show that this, together with an empirical estimate of the radial profile of the ambient lateral pressure in the outer corona, implies that the CME plasmoid increases in heliocentric angular width, θ_{CME}, as it rises until (before or after reaching the outer corona) it attains a final maximum angular width, Final θ_{CME}, thereafter remaining roughly constant in angular width as it moves on out, remaining in balance with the decreasing lateral pressure of the ambient corona:

$$[B_{CME}]^2/8\pi \approx p_{Lat,Amb}, \quad (4)$$

when $\theta_{CME} \approx$ constant = Final θ_{CME} in the outer corona.

For a roughly spherical CME plasmoid, the frontal cross-sectional area (perpendicular to the radial direction), A_{CME}, is given approximately by

$$A_{CME} \approx [R\theta_{CME}(R)]^2, \quad (5)$$

where $\theta_{CME}(R)$ is the angular width of the plasmoid when the center of the plasmoid's bright core is at radial distance R (Figure 2). An estimate of the magnetic flux content of the CME is given by the product of this area and the root-mean-square magnetic field strength in the CME:

$$\Phi_{CME} \approx [R\theta_{CME}(R)]^2 B_{CME}(R). \quad (6)$$

We assume that by the time the center of the CME plasmoid is in the outer corona ($R > 2R_{Sun}$) it is fully formed, no longer appreciably gaining or losing magnetic flux by reconnection, so that, by conservation of frozen-in magnetic flux, Φ_{CME} is constant in the

outer corona. In this case, if beyond some radial distance in the outer corona θ_{CME} is constant, then beyond that distance Equation (6) approximately gives:

$$B_{CME} \propto 1/R^2. \quad (7)$$

Thus, for our CME model, if beyond some distance in the outer corona, (1) the CME is in lateral pressure balance with ambient corona, and (2) the angular width of the CME is constant with R, then from Equation (4) the ambient lateral pressure must decrease approximately as $(B_{CME})^2$ in Equation (7):

$$p_{Lat,Amb} \propto 1/R^4. \quad (8)$$

Conversely, if $p_{Lat,Amb}$ falls of as $1/R^4$, then from Equations (4) and (6), θ_{CME} is approximately constant with distance when the CME plasmoid has attained lateral pressure balance with the surrounding outer corona.

When the CME plasmoid has reached lateral pressure balance with the ambient outer corona, from Equation (4), $B_{CME} \approx [8\pi\ p_{Lat,Amb}]^{1/2}$, and if $\theta_{CME} \approx$ constant = Final θ_{CME}, then Equation (6) is expressed by

$$\Phi_{CME} \approx [(\text{Final } \theta_{CME})R]^2\ [8\pi\ p_{Lat,Amb}]^{1/2}. \quad (9)$$

If the lateral pressure in the outer corona does fall off as $1/R^4$, then

$$p_{Lat,Amb} = p^*[R_{Sun}/R]^4, \quad (10)$$

where p* is the value of lateral pressure given by extrapolation of $p_{Lat,Amb}$ in the outer corona down to the surface of the Sun. In this case, if p* can be estimated, then the magnetic flux content of the CME can be estimated from its final angular width in the outer corona:

$$\Phi_{CME} \approx [8\pi\ p^*]^{1/2}\ R^2_{Sun}\ [\text{Final } \theta_{CME}]^2. \quad (11)$$

If A_{Flare} is the area covered by the flare arcade after flare maximum, and B_{Flare} is the average magnetic field strength in this area, then

$$\Phi_{Flare} = A_{Flare}\, B_{Flare}. \quad (12)$$

With A_{Flare} expressed by its equivalent angular width, θ_{Flare}, defined by

$$A_{Flare} \equiv [\theta_{Flare}\, R_{Sun}]^2, \quad (13)$$

Equations (1), (11), and (12) give

$$B_{Flare} \approx [8\pi p^*]^{1/2}[(\text{Final } \theta_{CME})/\theta_{Flare}]^2. \quad (14)$$

Thus, the field strength B_{Flare} required for the CME explosion to have come from the flare site can be estimated from an estimate of p* and the observed final angular widths of the CME and its flare.

2.2. Lateral Pressure in the Outer Corona

Visible-light images of the corona from space-based coronagraphs, especially from SOHO (e.g., see the LASCO/C2 movies linked to the on-line SOHO LASCO CME Catalogue (Yashiro et al 2004)), as well as images taken from the ground during eclipses (e.g., Golub & Pasachoff 1997), show various streamers and plumes, many of which are discernible out to distances of many solar radii. These images show that these structures can have far from radial directions in the inner corona ($R < 2R_{Sun}$), but that by about $3R_{Sun}$ and beyond, in the absence of CMEs, practically all streamers and plumes are nearly radial, at all latitudes and for all phases of the solar cycle. This suggests that in nearly the entire steady outer corona (everywhere except perhaps at the current sheets in streamers), the magnetic field is combed out by the solar wind outflow to be nearly radial. If this field is strong enough, the magnetic pressure will keep the field laterally nearly uniform. That is, except in the variable small fraction of the outer corona where the lateral pressure is not dominated by the magnetic pressure (inside streamer stalks), the nearly radial magnetic field in the steady outer corona will have about the same strength at all latitudes and longitudes (Suess & Smith 1996; Suess & Nerney 2006), with the strength possibly waxing and waning over the solar cycle. In the approximation of a uniform radial magnetic field, the field strength in the outer corona, B_{OC}, is given by

$$B_{OC} = B^*[R_{Sun}/R]^2, \quad (15)$$

where B* is the field strength given by radial extrapolation of the radial field in the outer corona down to the surface of the Sun. The value of B* is the same at all latitudes and longitudes, but might be expected to vary with the phase and amplitude of the solar cycle.

In situ measurement of the interplanetary magnetic field by Ulysses during solar cycle 23 showed that the strength of the radial component of the field at 1 AU, B_R(1 AU), averaged over several solar rotations, was nearly constant with latitude from equator to pole, and was nearly constant over the rise of the cycle from its minimum phase to its maximum phase (Smith et al 2001). These observations indicate that the nearly radial field in the outer corona is indeed of about the same strength all around the Sun, and, somewhat surprisingly, hardly changes in strength over the solar cycle. A one-year running average of the Ulysses B_R(1 AU) values fluctuates around a value of about 3×10^{-5} G with a 1-σ variance of about 1×10^{-5} G: $B_R(1\text{ AU}) \approx (3\pm1) \times 10^{-5}$ G. By conservation of radial magnetic flux, the radial component of the interplanetary field can be extrapolated back to

the Sun to obtain an estimate of the strength of the radial magnetic field in the outer corona: from Equation (15),

$$B^* = B_{OC}[R/R_{Sun}]^2 = B_R(1\ AU)\,[1\ AU/R_{Sun}]^2, \qquad (16)$$

which, for $B_R(1\ AU) \approx 3 \times 10^{-5}$ G, gives

$$B^* \approx 1.4\ G. \qquad (17)$$

Thus, the observed radial component of the interplanetary magnetic field sets the strength of the radial magnetic field in the outer corona. The value of about 1.4 G for B* is weaker than practically all magnetic fields on the Sun that explode to produce CMEs: for even the weakest such fields, those in and around filaments and/or filament channels in quiet regions, the field strength is typically 5-10 G (Tandberg-Hanssen 1977). If the lateral pressure in the outer corona is mostly from the magnetic field, B* ≈ 1.4 G is consistent with the observation that CMEs are typically much larger in angular width than the underlying flare that is produced in tandem with the CME (e.g., Kahler 1992): as the CME-driving plasmoid explodes from the sheared-core arcade, because its magnetic field is initially much stronger than 1.4 G, it must expand to a much larger angular width to reach lateral pressure balance with the radial field in the outer corona.

For the magnetic field strength in the outer corona approximated by Equation (15) with B* = 1.4 G, the profile of magnetic pressure, $[B_{OC}]^2/8\pi$, in the outer corona (2-20 R_{Sun}) and its extrapolation down to the solar surface are shown in Figure 3. Also plotted in Figure 3 is an estimate of the profile of roughly the highest thermal plasma pressure expected in the corona over the course of a solar cycle: each circled point is the thermal pressure given by the electron density at solar maximum (listed in Allen 1973) for a coronal temperature of 10^6 K. For the estimated pressure profiles in Figure 3, the total lateral pressure is given within a factor of about 2 by the magnetic pressure alone throughout the outer corona (2-20 R_{Sun}), and within a factor of less than 2 in the lower outer corona (2-10 R_{Sun}). To the same degree, the pressure of the magnetic field in the relatively low-density, low-thermal-pressure regions outside of streamer stalks in the outer corona also sets the total lateral pressure in the high-density, high-thermal-pressure interiors of streamer stalks (Suess & Nernery 2006). Therefore, the estimated magnetic and thermal pressure profiles in Figure 3 indicate that throughout the outer corona to within a factor of about 2 or less the total lateral pressure is given by

$$p_{Lat,Amb} \approx [B_{OC}]^2/8\pi = ([B^*]^2/8\pi)[R_{Sun}/R]^4. \qquad (18)$$

That is, the lateral pressure in the outer corona falls off approximately as $1/R^4$. Consequently, when the CME plasmoid has reached lateral pressure balance with the surrounding outer corona, its angular width no longer increases with distance ($\theta_{CME} \approx$ constant = Final θ_{CME}), $p_{Lat,Amb}$ is given approximately by Equation (10) with $p^* = [B^*]^2/8\pi$,

and from Equation (11), the magnetic flux content of a CME can be estimated from B* and the CME's final angular width in the outer corona:

$$\Phi_{CME} \approx B^*[R_{Sun}]^2[\text{Final } \theta_{CME}]^2. \quad (19)$$

In this approximation, from Equation (14), the flare-site field strength required for the CME to have exploded from the flare site is given by

$$B_{Flare} \approx B^*[(\text{Final } \theta_{CME})/ \theta_{Flare}]^2. \quad (20)$$

3. APPLICATION OF THE MODEL TO OBSERVED CORONAL MASS EJECTIONS

In this Section we apply our CME model to three selected CME events in which the CME occurred together with a flare. The main reasons for selecting these three events are the following. First, from the synchrony of the flare with the CME onset and from the magnetic setting of the flare and its location relative to the CME, the flare site was apparently the source of the magnetic explosion that drove the CME. Second, the flare was located near the limb, which indicates that the CME was viewed nearly side-on by LASCO and hence that the CME's apparent heliocentric angular width was its actual angular width. Finally, we chose our events to sample a wide range of source-flare areas and field strengths. Two of the events were selected because we had previously studied them; the third event was selected because its CME and flare are among the largest and strongest on record. For each event, from the measured final angular width of the CME (Final θ_{CME}) and the measured or estimated effective angular width of the flare (θ_{Flare}), we use Equation (20) to obtain an estimate of the flare-site field strength (B_{Flare}) required for the CME to have exploded from the flare site. We then consider whether this estimated required field strength is about the field strength expected for the magnetic setting of the flare, that is, whether the strength of the actual field at the flare site was appropriate for the CME to have exploded from the flare site.

Our three events and their pertinent quantities are listed in Table 1. A LASCO snapshot of each CME is shown in Figure 4. The first event is the Moore & Sterling (2007) streamer-puff CME of 2002 May 20, discussed in the Introduction. Its coronal dimming footprint supports the magnetic-arch-blowout picture for streamer-puff CMEs, but the candidate source flare's small span (~ 20 times smaller than the CME in angular width) presses the question of whether the magnetic field that exploded to produce this flare was large enough to have been the source of the CME's driving plasmoid. In the second event, the CME apparently came from the quiet-region filament-eruption magnetic explosion of 1999 February 9 studied by Sterling & Moore (2003). The third event is the large, fast CME from the X20 flare explosion on 2003 November 4 in the huge δ-sunspot active region AR 10486 when this region was on the southwest limb. For the thousands of CMEs

observed in the outer corona by LASCO between 1996 and 2002, the average speed in the plane of the sky was 430 km/s (Yashiro et al 2004). Each of our three CMEs was faster than average, and each continued to accelerate in the outer corona (Table 1). The CME speed, acceleration, and final angular width in the outer corona were each greater for the second event than for the first, and were each much greater yet for the third event (Table 1 and Figure 4).

For each CME, the LASCO image in Figure 4 shows the CME after it had attained its final angular width. The streamer-puff CME showed a fragmented bright outer envelope that was partly separated from the interior of the CME plasmoid by a thin dim gap (Figure 4, left panel). This suggests to us that in this CME the thin dim gap was the outer edge of the driving plasmoid and the bright envelope was the plug of inner corona that was pushed out ahead of and around the driving plasmoid. The CME of the second event was somewhat similar to that of the first event in showing a ragged version of the classic three-part bubble structure sketched in Figure 2. This is more evident in images earlier than the one in Figure 4 (middle panel). In this later image, the dim gap between the outer bright envelope and bright filament material in the driving plasmoid can be seen only on the equatorward side of the CME. In the non-differenced image of the large, fast CME (Figure 4, third panel), there is little evidence of three-part bubble structure, but the roughly circular outline is consistent with a roughly spherical magnetic bubble. To this degree, in each of our three events, the CME roughly fit the "spherical-plasmoid-with-legs" form sketched in Figure 2, and the CME's angular width θ_{CME} could be measured as indicated in Figure 2. In each image in Figure 4, the two radial lines are those that were used to define and measure the CME's angular width (θ_{CME}) in that image. For the first two CMEs, we used running-difference images as in Figure 4 to measure θ_{CME}, because these showed the side edges of the CME plasmoid more distinctly than did the non-differenced images. However, because our third CME was so large and strong that it strongly disturbed the surrounding outer corona, for this CME the non-differenced images showed the side edges of the CME plasmoid more distinctly than did the running-difference images. So, for the third CME, we measured θ_{CME} from the non-differenced images.

For each CME, we measured θ_{CME} and the radial distance R of the centroid of the CME plasmoid in the LASCO C2 and C3 coronagraph images in which the centroid was at or beyond the edge of the occulting disk, from as soon as possible until after the CME plasmoid had attained its final angular width and the width had either remained nearly constant for several consecutive images or the CME became too faint to measure. These measurements are plotted in Figure 5. The streamer-puff CME had already attained its final angular width of about 41° in the inner corona, before it emerged from behind the C2 occulting disk. When the filament-eruption CME of 1999 February 9 emerged from behind the C2 occulting disk, it was narrower than was the streamer-puff CME, but it continued to widen in the outer corona until it reached its final angular width of about 64° at a centroid distance of about 5 R_{Sun}. When the CME from the X20 flare emerged from the inner corona, it was already much wider than were either of the other two CMEs, and it continued to increase in angular width until, at and beyond a centroid distance of about 6 R_{Sun}, it attained and kept its Final θ_{CME} of about 128° (Figure 5 and Table 1). The observed

attainment of a persisting final angular width by each of our three CMEs agrees with the assumptions of our model CME and outer corona that (1) the magnetic pressure dominates the plasma pressure in the CME plasmoid and in the ambient outer corona, (2) when there is no CME present, the magnetic field in the outer corona is approximately uniform and radial, and (3) the CME plasmoid expands laterally until it attains and keeps lateral pressure balance with the magnetic field in the outer corona.

From Equation (19) with B* = 1.4 G and Final θ_{CME} in radians, the CME's estimated magnetic flux content, given by the measured value of Final θ_{CME} given above and in Table 1, is 3.5 x 10^{21} Mx for the first CME, 8.7 x 10^{21} Mx for the second CME, and 3.5 x 10^{22} Mx for the third CME. The magnetic flux content of a medium-sized active region is ~ 10^{22} Mx (Martres & Bruzek 1977; Fisher et al 1998). So, the estimated flux in the first CME seems perhaps somewhat large, but not obviously too large, for the CME to have exploded from a small part of a normal-sized active region, as was apparently the case (Moore & Sterling 2007). On the same basis, the estimated flux content of the second CME is of a reasonable magnitude for the CME to have exploded from a quiet-region sheared-core arcade that was many times larger in area than the largest active regions. The estimated flux in the third CME, though impressively large, is not too large for the CME to have exploded from AR 10486, which had a total magnetic flux of about 5 x 10^{22} Mx (measured from a Marshall Space Flight Center vector magnetogram taken on 2003 October 29, when the active region was at central meridian (Falconer 2006)).

For the streamer-puff CME of 2002 May 20, the candidate source explosion was a compact ejective flare in a small part of a growing active region near the southeast limb (the flare was at about S20°, E65°). The SOHO/EIT Fe XII movie captured a dark surge or spray, at the base of which was a compact area of bright emission. Registration of the Fe XII images with a SOHO/MDI magnetogram showed that the flare was seated on the neutral line of a small (~ 10^4 km diameter) δ sunspot inside the active region (Moore & Sterling 2007). Consistent with the small lateral extent (~ 10^4 km) of the flare emission and the large strength (~ 10^3 G) of the magnetic field in sunspots, the eruption produced a short-lived (1 hr) but exceptionally strong (GOES X1) X-ray burst. We measured the apparent (plane-of-the-sky) area of the flare emission in the EIT Fe XII image taken at 15:36 UT, early in the decay phase of the GOES X-ray burst. By assuming that this area was the flare-covered solar surface area A_{Flare} viewed in projection, we obtained $A_{Flare} \approx 7.3 \times 10^8$ km^2, the equivalent angular width of which is $\theta_{Flare} \approx 2.2°$ (Equation (13)).

Equation (20) with B* = 1.4 G, Final $\theta_{CME} = 41°$, and $\theta_{Flare} \approx 2.2°$, gives $B_{Flare} \approx 490$ G for the flare-site field strength required for the streamer-puff CME's driving plasmoid to have exploded from the compact ejective flare. This field strength is appropriate for a sheared-core magnetic arcade formed by the emergence of the magnetic field of a δ sunspot. That is, the candidate pre-eruption arcade quite plausibly contained enough magnetic flux for its eruption to produce an exploding flux-rope plasmoid that was strong enough and large enough to drive the observed CME. Thus, the estimated B_{Flare} supports the magnetic-arch-blowout scenario for the streamer-puff CME of 2000 May 20.

According to the magnetic-arch-blowout scenario, the 2000 May 20 streamer-puff CME was driven by a plasmoid that exploded from the ejective flare. The driving plasmoid

overpowered the large filament-holding arcade's outer loop that had the ejective flare in one foot, and drove out the top of this loop, making the loop top the outer envelope of the CME. This "opening" of the outer loop resulted in the coronal dimming observed in both ends of the loop (Moore & Sterling 2007). As we noted in Section 2.1, for this scenario to be plausible, the driving plasmoid should have contained more flux that did the outer loop that it overpowered. In the same way as we measured the area A_{Flare} covered by bright flare emission in the 15:36 UT image, in this same image (shown in Figure 3 of Moore & Sterling 2007) we measured the area A_{Foot} of the coronal dimming in the remote (non-flare) foot of the outer loop. We obtained $A_{Foot} \approx 8 \times 10^{19}$ cm^2. The noise level in MDI magnetograms is about 20 G (Scherrer et al 1995). In the registered MDI magnetogram, only a few percent of the remote dimmed area had detectable magnetic flux. So the average field strength in the area was evidently less than 20 G, as is normal for high-latitude quiet regions. Because this large quiet-region arcade held a filament in its sheared core field, from Tandberg-Hanssen (1977) we adopt a representative strength of 7.5 G for the magnetic field in this arcade. This gives about 6×10^{20} Mx for the magnetic flux Φ_{Foot} in the area A_{Foot} of the remote end of the outer loop. Hence, the total magnetic flux, $\Phi_{Loop} = 2\Phi_{Foot}$, in both legs of the large loop that was opened in the production of the CME was about 1.2×10^{21} Mx. From this estimate, we conclude that the magnetic flux in the opened outer loop was plausibly less than half of the total magnetic flux of 3.5×10^{21} Mx estimated for the CME from its final angular width. Thus, the amount of magnetic flux that was covered by the remote coronal dimming is consistent with the magnetic-arch-blowout scenario for this streamer-puff CME. This agreement and the agreement of the estimated and expected field strength at the flare support the CME model that we use to estimate Φ_{CME} and B_{Flare}, because the magnetic-arch-blowout scenario is a version of our CME model.

For our CME of 1999 February 9, the source of the driving explosion was evidently a quiet-region filament eruption that was centered at about N40°, E60°, and began its explosive phase at about 1:00 UT. This eruption produced no X-ray burst that rose above background in the GOES X-ray flux plot. However, a post-eruption long-duration flare arcade is obvious in Yohkoh/SXT full-disk coronal X-ray images. These images show that the flare arcade reached its maximum span near 12:00 UT. By measuring the lateral extent of the arcade in the image taken at 11:58 UT, we obtained the de-projected area A_{Flare} covered by the arcade, finding $A_{Flare} \approx 1.1 \times 10^{11}$ km^2, the equivalent angular width for which is $\theta_{Flare} \approx 27°$. Equation (20) then gives $B_{Flare} \approx 8$ G for the field strength required in the pre-eruption filament and arcade for the filament-eruption explosion to have been the source of the CME. This estimated required field strength is in the 5-10 G range of quiet-region filaments (Tandberg-Hanssen 1977). This agreement supports the basic tenets on which the estimate is based, namely (1) the final angular width of a CME in the outer corona gives a good estimate of magnetic flux content of the CME, and (2) the magnetic flux in a CME that explodes from a sheared-core arcade approximately equals the magnetic flux covered by the full-grown post-eruption flare arcade.

Our large, fast CME of 2003 November 4 obviously came from the X20 flare explosion that began about 19:30 UT in the large δ-sunspot active region AR 10486, which was 20°

south on the west limb. In contrast to the flares in our other two events, which were on the disk near the limb, this flare was on the limb, the flare arcade was viewed from the side, and the area spanned by the arcade could not be measured. In the EIT Fe XII movies, the extent of this flare arcade along the limb in the decay of the GOES X-ray burst was comparable to the length of the flare arcade in the decay phase of the X17 flare that occurred in AR 10486 on 2003 October 28 (beginning about 11:00 UT), when the active region was near central meridian. So, to obtain a rough estimate of the area covered by the X20 flare arcade, we measured the area covered by the X17 flare arcade in the EIT Fe XII image (taken at 12:24 UT) that best showed the full-grown flare arcade in the decay phase of the X17 GOES X-ray burst. This gave $A_{Flare} \approx 1.1 \times 10^{10}$ km^2, and $\theta_{Flare} \approx 8.7°$. With Final $\theta_{CME} = 128°$ and B* = 1.4 G, Equation (20) then gives $B_{Flare} \approx 300$ G for the estimated field strength required in the pre-eruption sheared-core arcade in AR 10486 on November 4 for the CME of November 4 to have exploded from there. The X17 flare arcade centered on the complex giant δ sunspot in AR 10486, straddling a neutral line that ran through the δ sunspot. The X20 flare arcade centered on the latitude of the δ sunspot and was of about the same length as the X17 flare arcade, so it seems likely that it straddled the same neutral line. In both flares, the arcade was about twice longer than the diameter of the δ sunspot; each end of the arcade was rooted in the outskirts of the active region, well outside the δ sunspot. The field strength inside sunspots is ~ 1000 G (Allen 1973), whereas the field strength averaged over the entire (sunspot and non-sunspot) area of an active region is ~ 100 G (e.g., Warren & Winebarger 2006). So, it is quite plausible that the average strength of the magnetic field in the pre-eruption sheared-core arcade for the X20 flare explosion was of order 300 G. Thus, to about the same degree as in our other two events, we find good agreement between the estimated and expected CME-source field strength in this large active-region event. This agreement for this exceptionally large and strong CME explosion further supports the model CME and outer corona that we use to estimate Φ_{CME} and B_{Flare}.

4. DISCUSSION

Each or our three CMEs apparently exploded from a very different flaring source magnetic field: one from a small δ sunspot in an active region, one from a large quiet-region filament-holding magnetic arcade, and one from a monster δ sunspot. Each CME expanded to a final maximum and constant heliocentric angular width in the outer corona. In each case we have tested whether this behavior could be explained by a simple plasmoid CME model in which a flux-rope plasmoid erupts from the flare site, driven by its magnetic pressure, and expands in angular width as it rises until it reaches lateral pressure equilibrium with the surrounding coronal magnetic field, becoming a roughly spherical plasmoid that drives the CME, fills most of the CME, and has constant angular width in the outer corona. This model, together with an empirical estimate (from the measured radial component of the interplanetary field) of the nearly radial magnetic field that dominates the total pressure in the outer corona, yields simple formulas for estimating the magnetic flux

content of the CME from its final angular width in the outer corona, and for estimating the field strength at the flare site from the CME's final angular width and the angular width of the area covered by the post-eruption flare arcade. In each of our three test cases, judging from the observed magnetic location of the flare site, the estimated CME flux content and flare-site field strength are in reasonable agreement with the expected flux content and strength of the field spanned by the flare arcade. This agreement for all three widely different sources of the driving explosion roughly validates the plasmoid CME model and the radial-field model outer corona used to estimate the CME flux content and flare-site field strength.

For the 2002 May 20 streamer-puff CME, the timing and magnetic arrangement of the compact ejective flare, the CME, and its coronal dimming footprint verify the magnetic-arch-blowout scenario proposed by Bemporad et al (2005) for streamer-puff CMEs, provided it is plausible that the flare explosion ejected a flux-rope plasmoid that had enough magnetic flux to produce the observed CME. Our test of this question for this event shows that it is indeed plausible for the observed CME to have exploded from the observed compact ejective flare. This further verifies the magnetic-arch-blowout scenario for streamer-puff CMEs.

In streamer-puff CMEs, in the outer corona, the CME is centered on the streamer and moves radially out along it, but the source of the driving explosion is in the foot of an outer loop of the arcade base of the streamer (Bemporad et al 2005; Moore & Sterling 2007). That is, the radial path of the CME in the outer corona is laterally offset from the source of the explosion. In the magnetic-arch-blowout scenario, this occurs because low in the corona the streamer-arcade field is strong enough to guide the driving plasmoid and laterally deflect it as it explodes up the leg of the arcade's outer loop that has the ejective flare in its foot. Streamer-puff CMEs are typically rather narrow (angular width $<\sim 30°$). [This is reasonable in light of our results: streamer-puff CMEs are narrow because of the limited magnetic flux content possible for a driving magnetic plasmoid produced by the explosion of a very compact sheared-core arcade.] However, it is well known that many much larger CMEs are also laterally offset from a flare that is produced together with the CME (Harrison 2006). Moore & Sterling (2007) propose that streamer-puff CMEs are one variety of a broader class of CMEs (which they call over-and-out CMEs) that are similarly laterally offset from their explosion source via guiding/deflection of the driving plasmoid by the surrounding coronal magnetic field in which the exploding field is embedded. They point out that the evidence provided by streamer-puff CMEs for the magnetic-arch-blowout scenario favors the view (e.g., Moore & Sterling 2006) that all magnetically driven CMEs, including all over-and-out CMEs, explode from sheared-core magnetic arcades. The CME model and results of the present paper further support this view.

Each of our three CMEs continued to accelerate in the outer corona before and after attaining its final angular width. In our model CME, the CME is accelerated by its own magnetic field pushing against the surrounding magnetic field. Because the ambient magnetic field in the outer corona is radial, the push of the CME's magnetic pressure against this field results in a radial outward force on the CME plasmoid. The magnetic tension of the legs of the CME plasmoid, the weight of the plasma in the CME, and the

drag force of the surrounding corona on the outward moving CME oppose the outward push of the CME's magnetic pressure, and if together they are greater than the outward push, the CME decelerates, as is often observed in the outer corona (Yashiro et al 2004). In each of our three CMEs, the outward push was evidently greater than the total retarding force when the CME was in the outer corona.

The success of our CME model in yielding correct estimates of the strength of the magnetic field in the source of the CME explosion indicates that this model is essentially the correct physical picture for CME explosions. This means that whether the explosion of a sheared-core arcade becomes a CME, and, if it does, the acceleration history of the CME after the driving plasmoid begins to erupt, are determined mainly by whether and how the plasmoid's internal magnetic pressure overcomes both the magnetic tension of the plasmoid's legs and the retarding magnetic pressure and tension of the surrounding magnetic field in which the arcade is embedded. That is, our results suggest that the production and direction of a CME (i.e., whether a CME occurs and whether the CME explodes nearly radially outward from its source site or is an over-and-out CME) depend as much on the strength and configuration of the magnetic field in which the exploding arcade is embedded as on the size and strength of the driving flux-rope plasmoid. The breakout-reconnection scenario for CME production proposed by Antiochos (1998) explicitly recognizes the importance of the magnetic field in which the sheared-core arcade is embedded, for the case in which the field arrangement is such that there is a reconnection site between the envelope of the sheared-core arcade and overarching field. Our model and results accommodate the breakout situation. Moreover, our results suggest that the surrounding field plays a nearly equally important role in the production of CMEs in all cases, whether or not the field arrangement allows breakout reconnection: if, in any way, the surrounding field allows the flare-producing magnetic explosion to eject a flux-rope plasmoid that escapes out through the corona to drive a CME, this driving plasmoid accelerates by pushing against its magnetic surroundings and expands laterally until it attains lateral pressure balance with the ambient coronal magnetic field.

For CMEs that are produced in tandem with a flare, as in our three example events, from Equations (1) and (19), the final angular width of the CME can be estimated from the magnetic flux covered by the full-grown flare arcade:

$$\text{Final } \theta_{CME} \approx [\Phi_{Flare}/B^*]^{1/2}[R_{Sun}]^{-1}. \qquad (21)$$

Because each of our example CMEs exploded from on or near the limb, the final angular width of the CME could be accurately measured from LASCO images, but the magnetic flux under the flare arcade could not be measured, even to order of magnitude, from MDI magnetograms. So, for our events, we could not evaluate the accuracy to which Equation (21) estimates the final angular width of CMEs. However, when the recently launched pair of STEREO spacecraft reach large angles from the Sun-Earth direction, their coronagraphs will view nearly from the side CMEs that explode from magnetic arcades that, viewed from Earth, are well away from the limb, and hence for which ground-based or near-Earth space-based magnetographs (MDI, Hinode, SDO) will be able to reasonably accurately measure

the magnetic flux spanned by the flare arcade. This will allow the accuracy of Equation (21) to be determined. If Equation (21) proves to be accurate enough, then for a CME that explodes from the face of the Sun viewed from Earth, the measured magnetic flux spanned by the CME's flare arcade will be a useful indicator of whether the CME is wide enough to hit the Earth. In this respect, our results are promising for forecasting of space weather in and near the Earth's magnetosphere.

REFERENCES:

Allen, C. W. 1973, Astrophysical Quantities (London: Athlone).

Antiochos, S. K. 1998, ApJ, 502, L181.

Antiochos, S. K., Dahlburg, R. B., & Klimchuk, J. A. 1994, ApJ, 420, L41.

Canfield, R. C., Hudson, H. S., & McKenzie, D. E. 1999, GRL, 26, 627.

Choudhary, D. P., & Moore, R. L. 2003, GRL 30, 2107.

Falconer, D. A. 2006, private communication.

Fisher, G. H., Longcope, D. W., Metcalf, T. R., & Pevtsov, A. A. 1998, ApJ, 508, 885.

Gibson, S. E., Foster, D., Burkepile, J., de Toma, G., & Stanger, A. 2006, ApJ, 641, 590.

Golub, L., & Pasachoff, J. M. 1997, The Solar Corona (Cambridge: Cambridge University Press).

Gopalswamy, N., & Thompson, B. J. 2000, Journal of Atmospheric and Solar-Terrestrial Physics, 62, 1457.

Gosling, J. T. 1993, JGR, 98, 18937.

Hagyard, M. J., Moore, R. L., & Emslie, A. G. 1984, Adv. Space Res., 4(7), 71.

Harrison, R. A. 1995, Astron. Astrophys., 304, 585.

Harrison, R. A. 2006, in Solar Eruptions and Energetic Particles, ed. N. Gopalswamy, R. Mewaldt, & J. Torsti (Washington, D. C.: AGU), 73.

Heyvaerts, J., Priest, E. R., & Rust, D. M. 1977, ApJ, 216, 123.

Howard, R. A., Sheeley, N. R., Jr., Koomen, M. J., & Michels, D. J. 1985, JGR, 90, 8173.

Hudson, H. S. 2000, ApJ, 531, L75.

Hudson, H., Haisch, B., & Strong, K. T. 1995, JGR, 100, 3473.

Kahler, S. W. 1992, ARAA, 30, 113.

Kahler, S. W. 2006, in Solar Eruptions and Energetic Paricles, ed. N. Gopalswamy, R. Mewaldt, & J. Torsti (Washington, D. C.: AGU), 21.

Kopp, R. A., & Pneuman, G. W. 1976, Sol. Phys., 50, 85.

Low, B. C. 1996, Sol. Phys., 167, 217.

Machado, M. E., Moore, R. L., Hernandez, A. M., Rovira, M. G., Hagyard, M. J., & Smith, J. B., Jr. 1988, ApJ, 326, 425.

Martres, M. J., & Bruzek, A. 1977, in Illustrated Glossary for Solar and Solar-Terrestrial Physics, ed. A. Bruzek & C. J. Durant (Dordrecht: Reidel), 53.

Moore, R. L. 1987, Sol. Phys., 113, 121.

Moore, R. L. 1988, ApJ, 324, 1132.

Moore, R. 2001, in Encyclopedia of Astronomy and Astrophysics, ed. P. Murdin (Bristol: Inst. Phys. Publ., 2691.

Moore, R., et al 1980, in Solar Flares, ed. P. A. Sturrock (Boulder: Colorado Associated University Press), 341.

Moore, R. L., Falconer, D. A., Porter, J. G., & Suess, S. T. 1999, ApJ, 525, 505.

Moore, R. L., Hagyard, M. J., & Davis, J. M. 1987, Sol. Phys., 113, 347.

Moore, R. L., Hagyard, M. J., Davis, J. M. & Porter, J. G. 1991, in Flare Physics in Solar Activity Maximum 22, ed. Y. Uchida, R. C. Canfield, T. Watanabe, & E. Hiei (Berlin: Springer-Verlag), 324.

Moore, R. L., Hurford, G. J., Jones, H. P., & Kane, S. R. 1984, ApJ, 276, 379.

Moore, R. L., & LaBonte, B. J. 1980, in Solar and Interplanetary Dynamics, ed. M. Dryer & E. Tandberg-Hanssen (Dordrecht: Reidel), 207.

Moore, R. L., LaRosa, T. N., & Orwig, L. E. 1995, ApJ, 438, 985.

Moore, R., & Rabin, D. 1985, ARAA, 23, 239.

Moore, R. L., & Roumeliotis, G. 1992, in Eruptive Solar Flares, ed. Z. Svestka, B. V. Jackson, & M. E. Machado (Berlin: Springer-Verlag), 69.

Moore, R. L., Schmieder, B., Hathaway, D. H., & Tarbell, T. D. 1997, Sol. Phys., 176, 153.

Moore, R. L., & Sterling, A. C. 2006a, in Solar Eruptions and Energetic Particles, ed. N. Gopalswamy, R. Mewaldt, & J. Torsti (Washington, D. C.: AGU), 43.

Moore, R. L. & Sterling, A. C. 2007, ApJ, submitted.

Moore, R. L., Sterling, A. C., Hudson, H. S., & Lemen, J. R. 2001, ApJ, 552, 833.

Plunkett, S. P., Thompson, B. J., St. Cry, O. C., & Howard, R. A. 2001, Journal of Atmospheric and Solar-Terrestrial Physics, 63, 389.

Rust, D. M., & Kumar, A. 1996, ApJ, 464, L199.

Rust, D. M., & LaBonte, B. J. 2005, ApJ, 622, L69.

Scherrer, P. H. 1995, Sol. Phys., 162, 129.

Shibata, K. 1998, in Observational Plasma Astrophysics: Five Years of Yohkoh and Beyond, ed. T. Watanabe, T. Kosugi, & A. C. Sterling (Dordrecht: Kluwer), 187.

Shibata, K., Masuda, S., Shimojo, M., Hara, H., Yokayama, T., Tsuneta, S., Kosugi, T., & Ogawara, Y. 1995, ApJ, 451, L83.

Smith, E. J., Balogh, A., Forsyth, R. J., & McComas, D. J. 2001, GRL, 28, 4159.

Sterling, A. C., Hudson, H. S., Thompson, B. J., & Zarro, D. M. 2000, ApJ, 532, 628.

Sterling, A. C., & Moore, R. L. 2001a, JGR, 106, 25227.

Sterling, A. C., & Moore, R. L. 2001b, ApJ, 560, 1045.

Sterling, A. C., & Moore, R. L. 2003, ApJ, 599, 1418.

Sterling, A. C., & Moore, R. L. 2004a, ApJ, 602, 1034.

Sterling, A. C., & Moore, R. L. 2004b, ApJ, 613, 1221.

Sterling, A. C., & Moore, R. L. 2005, ApJ, 630, 1148.

Sterling, A. C., Moore, R. L., & Thompson, B. J. 2001b, ApJ, 566, L219.

Sterling, A. C., Moore, R. L., Qiu, J., & Wang, H. 2001a, ApJ, 561, 1116.

Sturrock, P. A. (ed.) 1980, Solar Flares (Boulder: Colorado University Associated Press).

Sturrock, P. A., Kaufman, P., Moore, R. L., & Smith, D. F. 1984, Sol. Phys. 94, 341.

Suess, S. T., & Smith, E. J. 1996, GRL, 23, 3267.

Suess, S. T., & Nerney, S. 2006, GRL, 33, L10104.

Svestka, Z. 1976, Solar Flares (Dordrecht: Reidel).

Svestka, Z., Jackson, B. V., & Machado, M. E. (eds.) 1992, Eruptive Solar Flares (Berlin: Springer-Verlag).

Tandberg-Hanssen, E. 1977, in Illustrated Glossary for Solar and Solar-Terrestrial Physics, ed. A. Bruzek & C. J. Durant (Dordrecht: Reidel), 97.

Warren, H. P., & Winebarger, A. R. 2006, ApJ, 645, 711.

Yashiro, S., Gopalswamy, N., Michalek, G., St. Cyr, O. C., Plunkett, S. R., Rich, N. B., & Howard, R. A. 2004, JGR, 109, A07105.

Table 1 Measured Aspects and Estimated Magnetic Quantities in Three Observed CME Events						
Event[a]	CME Speed[b] (km/s)	CME Acceleration[b] (m/s^2)	Final θ_{CME} (deg)	θ_{Flare} (deg)	Φ_{CME} (10^{21} Mx)	B_{Flare} (G)
1	660	58	41	2.2	3.5	490
2	850	61	64	27	8.7	8
3	2700	430	128	8.7	35	300

[a] Event 1: 2002 May 20 streamer-puff CME from strong (GOES X1) compact ejective flare in small δ sunspot near limb. Event 2: 1999 February 9 CME from quiet-region filament eruption near limb. Event 3: 2003 November 4 CME from great (GOES X20) flare explosion in giant δ-sunspot active region at limb.

[b] From the SOHO LASCO CME Catalogue (Yashiro et al 2004).

Figure Captions

Figure 1. Depiction of the progression of the three-dimensional form and internal reconnection of the magnetic field in a sheared-core arcade as it explodes in either a confined (no-CME) eruption (lower left) or an ejective (CME-producing) eruption (lower right) (from Moore et al 2001).

Figure 2. Schematic of our "spherical-plasmoid-with-legs" model CME viewed in the outer corona beyond the 2 R_{Sun} occulting disk of LASCO/C2 when the radial distance R of the centroid of the CME (the center of the CME "sphere") is about 4 R_{Sun}.

Figure 3. Empirically estimated radial profiles of the magnetic pressure ($B^2/8\pi$) and thermal plasma pressure ($3n_ekT$) in the outer corona (2-20 R_{Sun}) (see text). The magnetic pressure dominates at distances of 2-10 R_{Sun} and is comparable to the plasma pressure at 10-20 R_{Sun}.

Figure 4. Snapshots of our three trial CMEs in the outer corona and at their final, maximum angular width. Left: LASCO/C2 running-difference image of the 2002 May 20 streamer-puff CME; final angular width: 41°. Middle: LASCO/C2 running-difference image of the 1999 February 9 quiet-region filament-eruption CME; final angular width: 64°. Right: LASCO/C3 image of the great active-region eruptive-flare CME: final angular width: 128°.

Figure 5. Observed progression of the angular widths of our three trial CMEs. The measured angular width θ_{CME} is the angle between two encompassing tangent radial lines, such as shown in Figure 4. The measured radial distance R of the "centroid" of the CME is the average of the radial distances of the two tangent points. The error bars are from the uncertainties in the lateral and radial locations of the tangent points.

Figure 1.

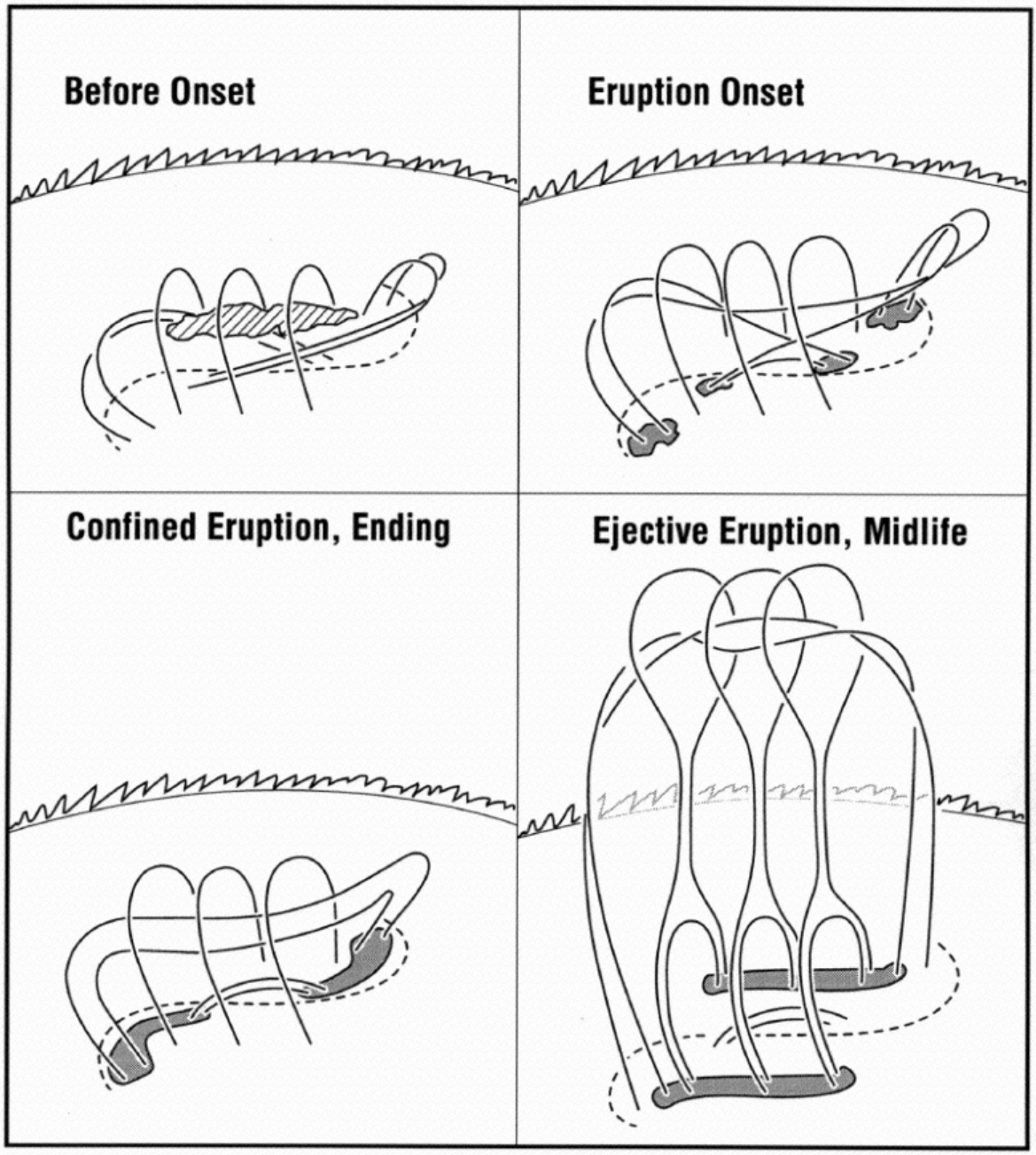
Before Onset
Eruption Onset
Confined Eruption, Ending
Ejective Eruption, Midlife

Figure 2.

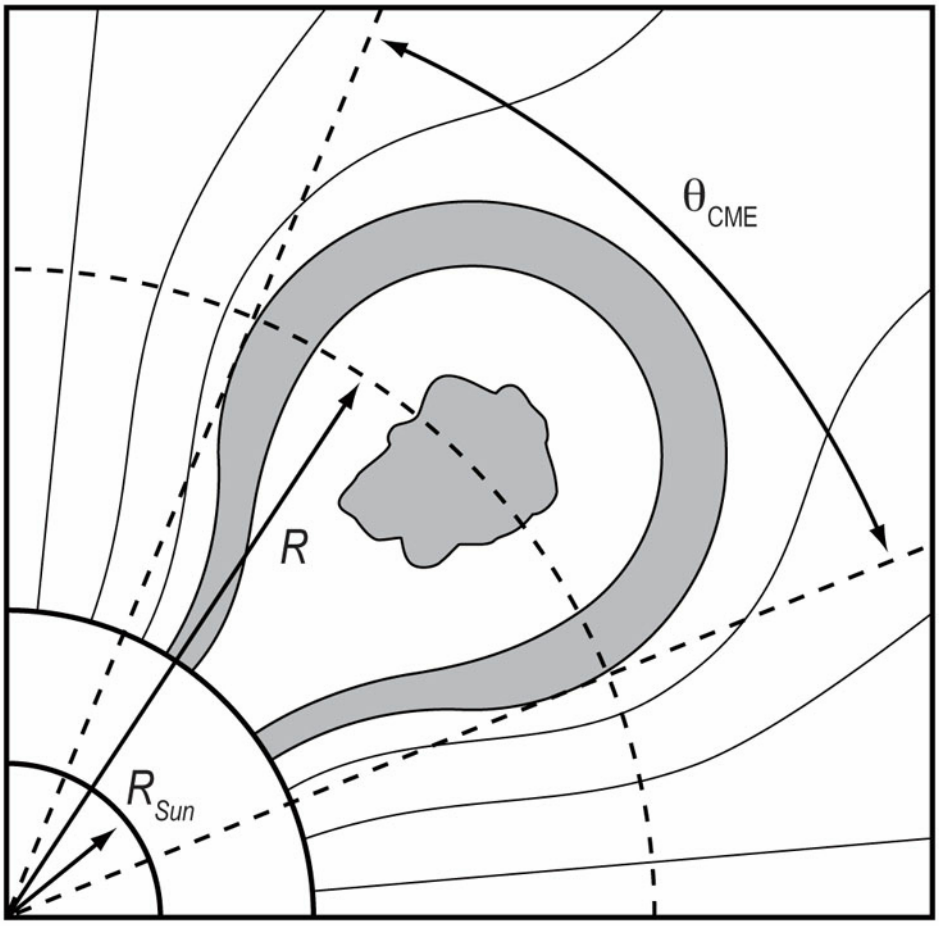

Figure 3.

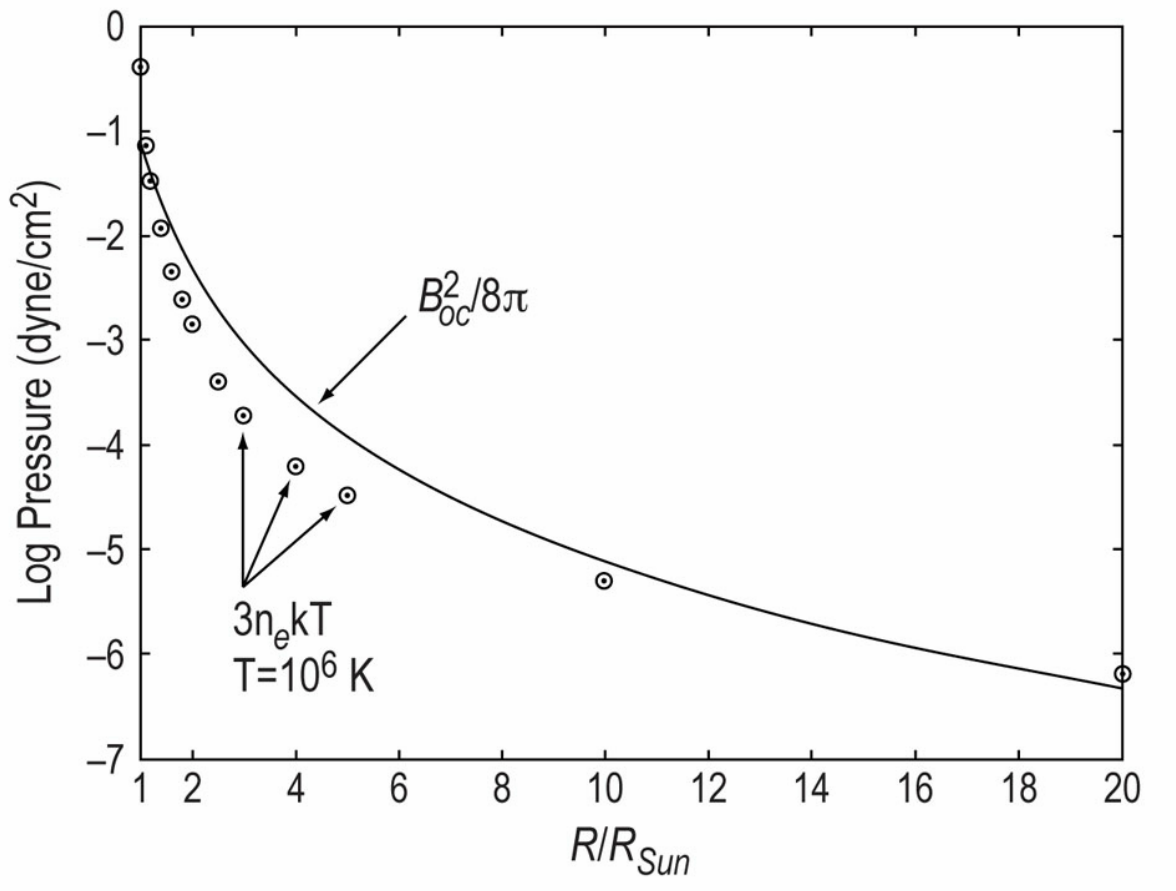
0
−1
−2
−3
−4
−5
−6
−7
Log Pressure (dyne/cm²)
$B_{oc}^2/8\pi$
$3n_ekT$
$T=10^6$ K
1
2
4
6
8
10
12
14
16
18
20
R/R_{Sun}

Figure 4.

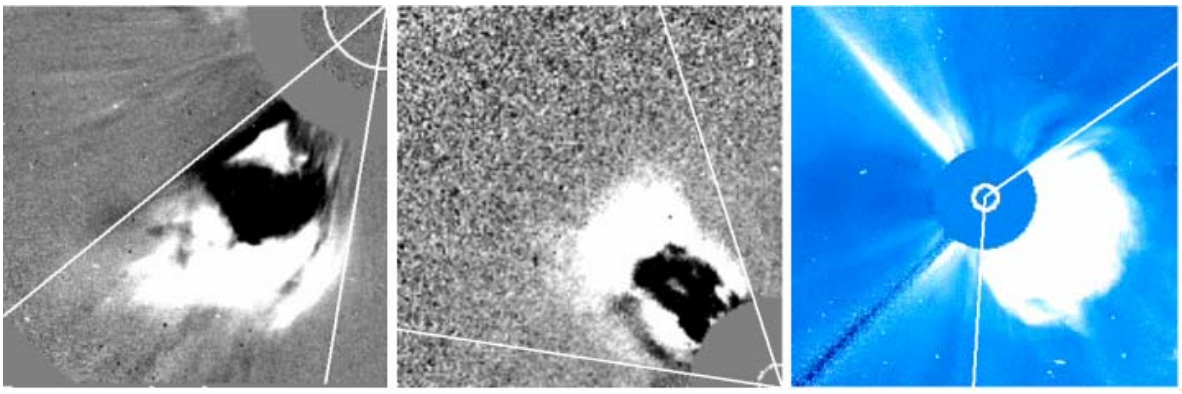

Figure 5.

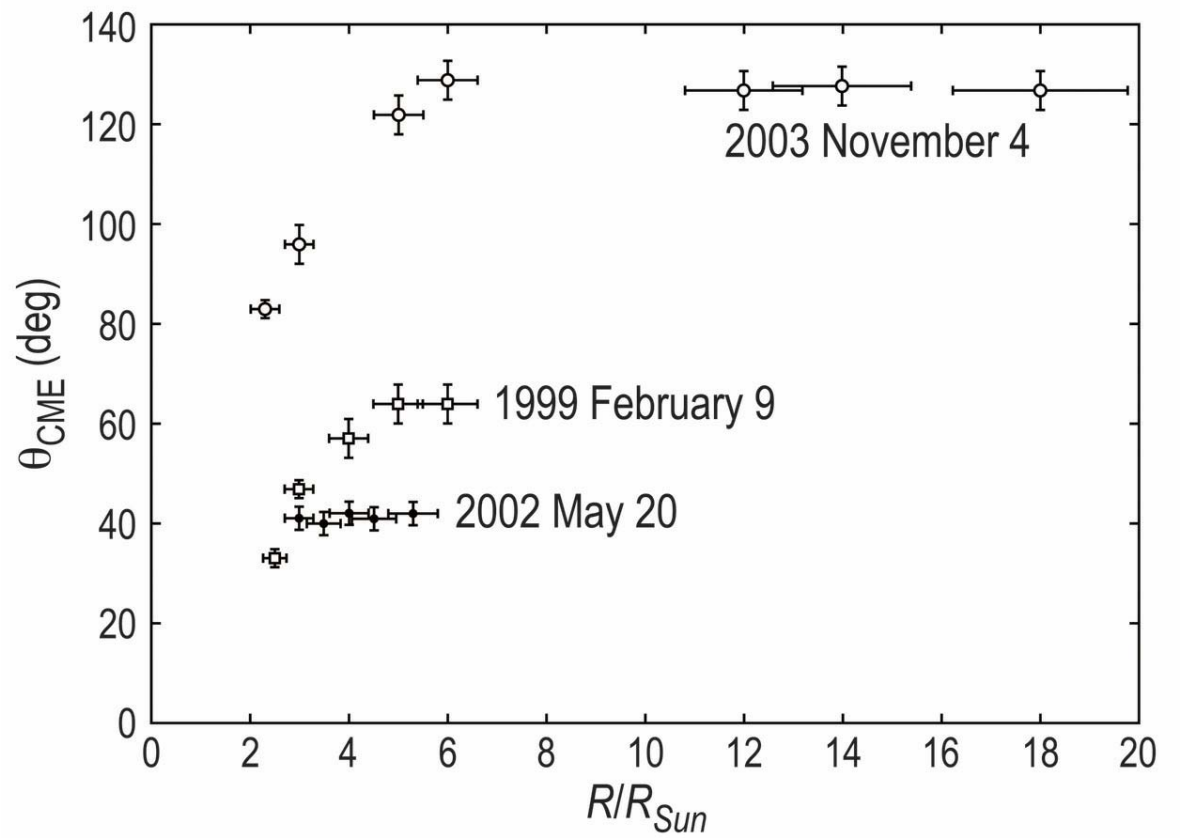
140
120
100
80
60
40
20
0
0
2
4
6
8
10
12
14
16
18
20
θCME (deg)
R/RSun
2003 November 4
1999 February 9
2002 May 20